A Selective Matrix Metalloprotease 12 Inhibitor for Potential Treatment of Chronic Obstructive Pulmonary Disease (COPD): Discovery of (S)-2-(8-(Methoxycarbonylamino)dibenzo[b,d]furan-3-sulfonamido)-3-methylbutanoic acid (MMP408)

Wei Li,*,[†] Jianchang Li,[†] Yuchuan Wu,[†] Junjun Wu,[†] Rajeev Hotchandani,[†] Kristina Cunningham,[†] Iain McFadyen,[†] Joel Bard,[†] Paul Morgan,[‡] Franklin Schlerman,[‡] Xin Xu,[§] Steve Tam,[†] Samuel J. Goldman,[‡] Cara Williams,[‡] Joseph Sypek,[‡] and Tarek S. Mansour[†]

Chemical Sciences, Inflammation, and Drug Safety and Metabolism, Wyeth Research, 200 Cambridge Park Drive, Cambridge, Massachusetts 02140

Received January 22, 2009

Abstract: Matrix metalloprotease 12 plays a significant role in airway inflammation and remodeling. Increased expression and production of MMP-12 have been found in the lung of human COPD patients. MMP408 (**14**), a potent and selective MMP-12 inhibitor, was derived from a potent matrix metalloprotease 2 and 13 inhibitor via lead optimization and has good physical properties and bioavailability. The compound blocks rhMMP-12-induced lung inflammation in a mouse model and was advanced for further development for the treatment of COPD.

Chronic obstructive pulmonary disease (COPD[a]) is a chronic progressive respiratory disease characterized by airflow limitation that is not fully reversible.[1] COPD is associated with an abnormal inflammatory response of the lung to noxious particles or gas, mainly caused by cigarette smoke. The disease ranks among the top five leading causes of death and is expected to grow because of increased prevalence with increasing age, cigarette smoking, and environmental factors.[2] Presently, there are only symptomatic therapies,[3] and no disease-modifying drugs are available for this indication.[4,5] Pathologic degradation of the extracellular matrix (ECM) of the bronchial wall may represent an important cause of airflow obstruction in COPD. Matrix metalloproteases (MMPs) have been suggested to be the major proteolytic enzymes to induce this progressive airway remodeling.[6]

MMP-12, in particular, has been shown to play a significant role in airway inflammation and remodeling. MMP-12 is the primary elastolytic enzyme of alveolar macrophages.[7] Preclinical studies in COPD/emphysema support blocking MMP-12 as a valid approach for therapeutic intervention. Specifically, MMP-
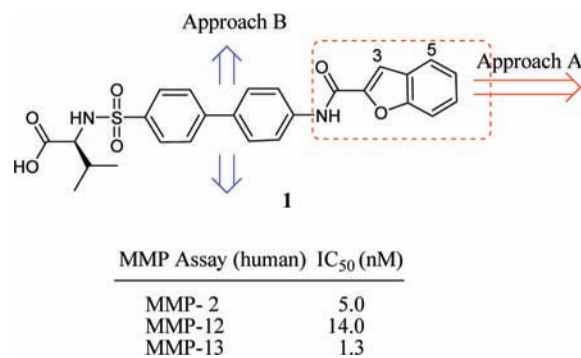
---

* To whom correspondence should be addressed. Phone: 1-617-665-5625. Fax: 1-617-499-1017. E-mail: weili@wyeth.com.
    † Chemical Sciences.
    ‡ Inflammation.
    § Drug Safety and Metabolism.
    [a] Abbreviations: MMP-12, matrix metalloprotease 12; ECM, extracellular matrix; MMP-13, matrix metalloprotease 13; MMP-2, matrix metalloprotease 2; COPD, chronic obstructive pulmonary disease; HTS, high-throughput screening; ZCG, zinc-chelating group; DBF, dibenzofuran; SAR, structure−activity relationship; PK, pharmacokinetics; HLM, human liver microsomes; MLM, mouse liver microsomes; hERG, human ether-a-go-go related gene; q.d., quaque die; b.i.d., bis in die; po, per os.

Figure 1. Two approaches for modification of the lead compound **1**.

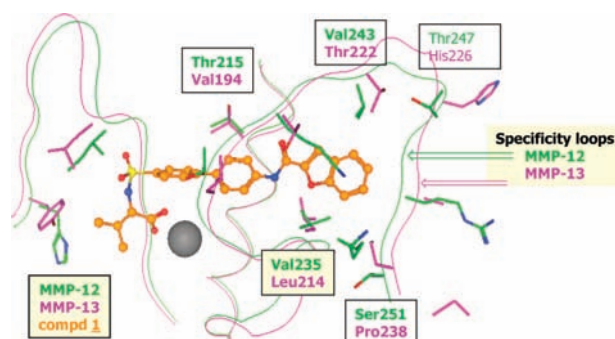| MMP Assay (human)	IC_{50} (nM)
MMP-2	5.0
MMP-12	14.0
MMP-13	1.3

Figure 2. Homology model indicates similar loops in shape and size for MMP-12 (green in color) and -13 (purple), which poses great challenges for selectivity.

12-deficient mice show significantly impaired macrophage and neutrophil recruitment in response to cigarette smoke[8,9] and markedly reduced TNF-α production.[10] Pathological evidence indicates that MMP-12-deficient mice are protected against the development of emphysema induced by cigarette smoke.[8]

Establishing high quality leads with attractive physical properties was the target at the inception of the program. In addition to mining hits generated from the HTS, activity and selectivity data generated by all of our in-house MMP programs were available to us. One structure in particular that drew our attention was **1**, a lead from the MMP-13 program (Figure 1).[11]

Compound **1** (Figure 1) is a potent MMP-2/-13 inhibitor with excellent MMP-12 activity (IC_{50} = 14 nM). As illustrated by the model shown in Figure 2, the carboxylic acid acts as a zinc-chelating group (ZCG) and the biphenyl rings sit in the S1′ pocket. The benzofuran attachment is located deep in the S1′ pocket close to the solvent front.

On the basis of the model, the specificity loops[12] of MMP-12, -13, and -2 (not shown) have great similarities in size and shape, with MMP-12 having the smallest among the three enzymes. For the MMP-13 program, the selectivity over MMP-2 and -12 was successfully achieved by increasing the number and size of the substituents at the C3 and C5 positions of the benzofuran so that they clash with the smaller loops of MMP-12 and -2 but not MMP-13.[13,14] Extending in that direction (approach A, Figure 1) would be not viable for the MMP-12 program, since the MMP-12 loop would be hit first before reaching to the loops of MMP-2 and -13.

On the other hand, approach B, which goes in the direction orthogonal to approach A, appeared to be very attractive.
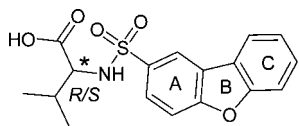
Table 1. Selectivity Achieved with DBF Analogues

| compd | IC$_{50}$ (nM) | | selectivity, MMP-12/-13 |
	MMP-12	MMP-13	
1	14	1.3	0.1
(*R*)-**2a**	38	2500	65
(*S*)-**2b**	600	25000	42

Molecular modeling indicated that there is a 30° dihedral angle between the two phenyl rings in **1**. The design of new scaffolds that change this dihedral angle or restrict the rotation of the biphenyl rings would be a novel approach. This could be accomplished by linking the biphenyl rings with a heteroatom to form a tricyclic core, effectively realizing the expansion at the S1′ pocket.

To our delight, the new molecules synthesized on the basis of a dibenzofuran (DBF) scaffold[15] achieved impressive selectivity over MMP-13 while maintaining decent MMP-12 activity (Table 1). By comparison to **1**, which favors MMP-13 over MMP-12, the new analogues showed better potency toward MMP-12 than MMP-13, a complete reversal of selectivity. Compound **2a** represents a true breakthrough in selectivity over MMP-13 with a remarkable 650-fold increase compared to **1**.

An aspect of chiral recognition is also observed. Similar to the trend in selectivity, the (*R*)-isomer exhibits better potency than the (*S*)-isomer. Although the MMP-12 potency of these analogues is weaker than that of **1**, further improvements could be achieved through chemical modification.

The X-ray cocrystal structure with the MMP-12 enzyme provided useful information for understanding the inhibitor−enzyme interaction and reliable information for modeling. For example, modeling suggested there was no space for substitution at the C1, C4, C6, and C9 positions along the spherical tricyclic core, which guided the efforts in SAR development to focus on the remaining positions C2, C3, C7, and C8. There are only four possible combinations of regioisomers given a set of substituents, namely, C2/C7, C2/C8, C3/C7, and C3/C8. The C2/C8 combination was ruled out as less favorable on the basis of modeling. The SAR development was thus focused on the remaining three combinations (Table 2).

Table 2 shows the results of SAR studies of the sulfonamide, carbamate, and urea analogues derived from the C-ring modification. As shown by the IC$_{50}$ values (average of multiple tests), potencies of some analogues increased to single digit nanomolar. For the sulfonamide derivatives, their potencies against MMP-12 spread from 10 nM to 2.5 μM favoring smaller alkyl groups on the sulfonamide. For example, potency was gained by 3.5-fold for **3a** compared to **2a** with an unsubstituted C-ring. The improved potency over the unsubstituted analogues indicates a favorable interaction of the sulfonamide moiety with the protein backbone in the deeper S1′ pocket. Similar chiral recognition is also observed. For example, the IC$_{50}$ of enantiomer (*R*)-**3a** is 16-fold more potent than (*S*)-**3b**, with the (*R*)-enantiomer being the favored configuration. Selectivity over MMP-13 was maintained. The best selectivity over MMP-13 among these sulfonamides is demonstrated by **3a** (100-fold) and **3b** (147-fold). It appears that there is little tolerance in regard to the size of the R group for these sulfonamide analogues, as the potency diminished dramatically with bigger R groups (**5**).

The SAR of the carbamate analogues is also well defined. Unlike the sulfonamides, the regioisomers with the C3/C8

Table 2. SAR of Sulfonamide, Carbamate, and Urea Analogues

| substituents | | | | | | IC$_{50}$ (nM) | |
A/C ring		R	X	Y	compd	MMP-12	MMP-13
C2	C7	methyl		SO$_2$	(*R*)-**3a**	11.0	1100
C2	C7	methyl		SO$_2$	(*S*)-**3b**	170.0	25000
C2	C7	isopropyl		SO$_2$	(*R*)-**4**	50.0	120
C2	C7	4-(3,5-dimethyl)isoxazole		SO$_2$	(*R*)-**5**	2500	34000
C2	C7	phenyl		SO$_2$	(*R*)-**6**	100	6000
C3	C8	methyl		SO$_2$	(*S*)-**7**	10.3	93
C3	C8	2,2,2-trifluoroethyl		SO$_2$	(*S*)-**8**	70.0	670
C2	C7	*O*-methyl		CO	(*R*)-**9**	7.2	500
C2	C7	*O*-*n*-propyl		CO	(*R*)-**10**	14.0	109
C2	C7	*O*-isopropyl		CO	(*R*)-**11**	39.0	500
C2	C7	*O*-phenyl		CO	(*R*)-**12**	45.0	600
C2	C7	*O*-methyl	8-Br	CO	(*R*)-**13a**	1050	25446
C2	C7	*O*-methyl	8-Br	CO	(*S*)-**13b**	3900	>25000
C3	C8	*O*-methyl		CO	(*S*)-**14**	2.0	120
C3	C8	*O*-ethyl		CO	(*S*)-**15**	5.0	100
C3	C8	*O*-*n*-propyl		CO	(*S*)-**16**	5.6	10
C3	C8	*O*-isobutyl		CO	(*S*)-**17**	4.7	10
C3	C8	*O*-(2-fluoro)ethyl		CO	(*S*)-**18**	2.1	10
C3	C8	*O*-phenyl		CO	(*S*)-**19**	10.2	220
C3	C8	*O*-(2-Cl)phenyl		CO	(*S*)-**20**	6.6	180
C3	C8	*O*-(4-F)phenyl		CO	(*S*)-**21**	8.1	200
C3	C8	*O*-(4-Me)phenyl		CO	(*S*)-**22**	14.0	100
C3	C8	NH$_2$		CO	(*S*)-**23**	7.6	59.0
C3	C8	*N*-cyclopentyl		CO	(*S*)-**24**	5.0	2.1
C3	C8	*N*-thiophen-3-yl		CO	(*S*)-**25**	0.9	3.3
C3	C8	N-(thiophen-2-yl)ethyl		CO	(*S*)-**26**	1.1	1.1
C3	C7	*O*-methyl		CO	(*S*)-**27**	12.0	>1000
C3	C7	*O*-(2-fluoro)ethyl		CO	(*S*)-**28**	10.0	97
C3	C7	*O*-(4-fluoro)phenyl		CO	(*S*)-**29**	16.0	361

combination (**14**−**22**) are more potent than those of C2/C7 (**9**−**13**). For example, the IC$_{50}$ of the C3/C8 isomer **14** is 2 nM, whereas the C2/C7 regioisomer methyl carbamate **9** is 7.2 nM. Similar results are observed for **10** and **16** (14.0 vs 5.6 nM, respectively). There is no tolerance toward ortho-substitution to the carbamate moiety, as an 8-Br substituent (**13a** and **13b**) dramatically reduced the potency compared to **9**. As to the potency of the C3/C7 regioisomers, they are also less potent in general than their C3/C8 counterparts. For example, the 2-fluoroethyl carbamate **18** (C3/C8) has an IC$_{50}$ value of 2.1 nM, whereas the C3/C7 isomer **28** experienced a 5-fold drop in potency to 10 nM.

However, the urea derivatives have activities different from those of the carbamates. The urea analogues (**23**−**26**) are very potent MMP-12 inhibitors but less selective over MMP-13. In fact, ureas **24**−**26** are nearly equipotent for MMP-12 and MMP-13, implicating similar interactions of the urea residues with the enzymes within the S1′ pocket of MMP-12 and MMP-13. There is also more tolerance toward bigger substituents on the urea nitrogen as shown by **25** and **26**.

It is interesting to note that among the three methyl carbamate regioisomers **9** (C2/C7), **14** (C3/C8), and **27** (C3/C7), **14** is the most potent (2 nM) with **9** and **27** being equally potent (12.0 nM).

Efficient, interrelated routes for preparation of the three key nitro-DBF sulfonyl chlorides **32**, **34**, and **36** were developed according to their defined regiocombinations (eqs 1−3, Scheme 1). For example, sulfonyl chloride **32** (C2/C7 combination) was prepared in two steps: nitration of DBF (**30**) generated the desired 3-nitrodibenzofuran (**31**) in 70% yield,[16] which was treated with chlorosulfonic acid to generate **32** (Scheme 1, reaction 1).

Table 3. Pharmacokinetic Data for Selected Compounds

compd	iv (mg/kg)	Vd_{ss} (L/kg)	CL ((mL/min)/kg)	po (mg/kg)	$T_{1/2}$ (h)	C_{max} (ng/mL)	AUC (h^ang/mL)	F (%)
3a	2	1.9	141.3	30	2.0	103	245	7
9	2	1.6	8.3	30	2.7	10583	21659	36
14	2	1.9	17.2	30	3.0	3084	7476	27
15	2	1.6	19.0	30	3.4	7791	10834	42
26	2	15.6	211.0	10	NA^a	NA^a	NA^a	

^{a} Systemic exposure was negligible.

Scheme 1. Preparation of the Key DBF Intermediates^a
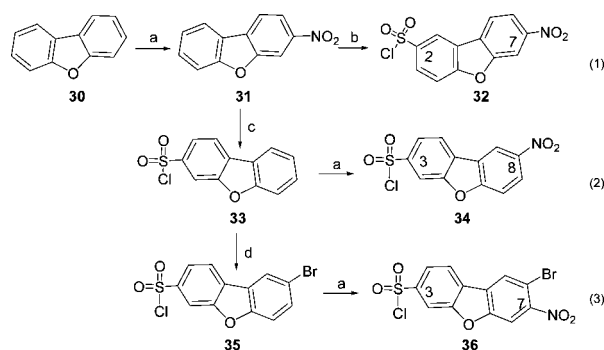
^{a} Reagents and conditions: (a) HNO_3, TFA (70−95%); (b) (i) HSO_3Cl in $CHCl_3$, 85%; (ii) $SOCl_2$, DMF (cat.) 90%; (c) (i) Pd/C, H_2, CH_3OH; (ii) $NaNO_2$, HCl; (iii) SO_2, CuCl, 74%; (d) Br_2, HOAc, 70 °C, 4 h, 80%.

Scheme 2. Preparation of Compound **14**^{a}

^{a} Reagents and conditions: (a) (L)-valine esters, TEA, in DCM, 94%; (b) Pd/C, H_2, MeOH, 98%; (c) methyl chloroformate, pyridine in DCM, 85%; (d) TFA/DCM, 98%.

Table 4. Cross-Species Activity and Selectivity Profile of **14**

MMP-12 IC_{50} (nM) of Different Species			
human	mouse	rat	sheep
2.0	160	320	22.3

IC_{50} (nM) of Other Human MMPs									
MMP-1	-3	-7	-9	-12	-13	-14	TACE	Agg-1	Agg-2
>6 μM	351	>22 μM	1300	2	120	1100	>25 μM	>5 μM	>10 μM

Preparation of the nitrosulfonyl chloride **34** required manipulations to generate the desired C3/C8 combination. The C3-sulfonyl chloride **33** was made through reduction of the −NO_2 in **31** to −NH_2, which was further transformed to the diazonium salt, followed by SO_2 treatment in the presence of CuCl.[17] The desired sulfonyl chloride **33** was treated with HNO_3 in TFA to afford the desired nitroarene **34** in very good yield (conditions c and a, Scheme 1). The different regiochemistry of the nitrations on **30** and **33** may be attributed to the influence of the electron-withdrawing sulfonyl chloride group in **33**, which directs the nitration to C8, furnishing **34**.

Preparation of the 8-bromo-7-nitrodibenzo[b,d]furan-3-sulfonyl chloride (**36**) required extensive manipulation to place the nitro group at the desired C7 position. Bromination is a necessary step to block the C8 carbon to generate **35** for the subsequent regioselective C7 nitration to obtain **36**. Removal of the bromo and reduction of −NO_2 to −NH_2 could be accomplished simultaneously via catalytic hydrogenation at a later stage (conditions d and a, Scheme 1).

As illustrated in Scheme 1, preparation of the three key intermediates is an integral chemistry effort for maximizing synthetic efficiency. Thus, the synthetic approaches to the less accessible and more complicated sulfonyl chlorides were designed to commence from the penultimates of the simpler ones (**31** for **34**, **33** for **36**). General procedures to progress from the sulfonyl chlorides to the final compounds are exemplified in Scheme 2.

Pharmacokinetic data (in C57BL/6 mice) indicate that carbamate analogues **9**, **14**, and **15** show better exposure and bioavailability than the sulfonamide **3a** and urea **26** (Table 3). Compound **3a** and **26** have high clearance rates (141.3 and 211.0 (mL/min)/kg, respectively) with low (**3a**) to very poor exposure (**26**). Compounds **3a**, **9**, and **14** were tested in a mouse lung inflammation model[18] (30 mg/kg, po), and compound **14**, (*S*)-2-(8-(methoxycarbonylamino)dibenzo[b,d]furan-3-sulfonamido)-3-methylbutanoic acid, showed the optimum in vivo efficacy and thus was advanced as MMP408 for further preclinical evaluation.[19]

Compound **14** was also profiled for cross-species MMP-12 activity and selectivity against other human MMPs (Table 4). Compared with human MMP-12, **14** has lower potency in rodent MMP-12 (80- and 160-fold less active for mouse and rat, respectively). This compound also maintains a good selectivity profile over other human MMPs.

In the metabolic stability studies carried out in the liver microsomal system, **14** appeared to be very stable in mouse, rat, dog, monkey, and human (in vitro $t_{1/2}$ > 60 min). An acylglucuronide was the only metabolite detected in all species at a very low level. Further in vitro metabolic stability of **14** was also determined in cryopreserved hepatocytes of dog, monkey, and human. In this system, metabolism of **14** was low to moderate in dog and very low in monkey and human. An aniline metabolite was detected in this hepatocyte study, which appears to be derived from the chemical degradation of the methyl carbamate moiety.

Further drug safety evaluations for **14** were performed with favorable results. For example, **14** exhibited a negative Ames test and has no hERG activity.

Scheme 2 illustrates the synthesis of **14**. The amino acid moiety of **14** was installed via coupling of the sulfonyl chloride **34** with (L)-valine *tert*-butyl ester in the presence of base to obtain **37**. The nitro group on the C ring of **37** was reduced to the corresponding aniline **38** in high yield via palladium catalyzed hydrogenolysis. Compound **38** was then derivatized
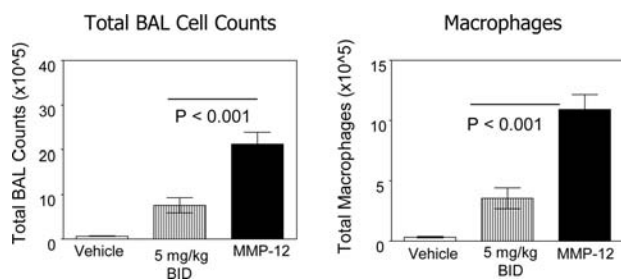
Figure 3. Oral efficacy of **14** in rhMMP-12 induced lung inflammation (5 mg/kg, b.i.d. po vs MMP-12 plus vehicle).

by treatment with methyl chloroformate in the presence of a mild base to generate the penultimate *tert*-butyl ester **39** in 85% yield.

The *tert*-butyl ester **39** was hydrolyzed under acidic conditions to generate the desired final product **14** with 73% overall yield from **34**. Originally, the (L)-valine methyl ester was used for the preparation of **14**. However, saponification of the corresponding methyl ester penultimate under basic conditions resulted in **14** but with contamination from the decomposition of the carbamate moiety. Thus, it was replaced with the *tert*-butyl ester. Chiral analysis of **14** confirmed that there was no impurity from epimerization of the chiral center during the synthesis.

To evaluate the compounds in vivo, an MMP-12 dependent pulmonary inflammatory response was induced in C57BL/6 mice by intranasal administration of recombinant human (rh) MMP-12[18] for 3 consecutive days. Inflammation within the bronchoalveolar lavage fluid was then quantified 24 h after the final dose of rhMMP-12. Compound **14** showed significant reduction in total BAL inflammation (>50% inhibition, $p < 0.001$) and absolute macrophages (>70% inhibition, $P < 0.001$) compared to rhMMP-12 plus vehicle alone when administered at 30 mg/kg (po, q.d.) 2 h prior to each of the 3 doses of rhMMP-12. Further studies determined that the minimum efficacious dose for **14** was 5 mg/kg (po, b.i.d.) in this model (Figure 3).

In summary, molecules with druglike properties for the MMP-12 program were obtained via modification of the potent MMP-13 inhibitor **1**. The key factor that reverses the selectivity profile of **1** is the replacement of the biphenyl core with the tricyclic scaffold, which also offers metabolic stability and good PK properties. Compound **14**, a potent, selective, and orally available MMP-12 inhibitor was identified. The demonstrated ability to attenuate pulmonary inflammation supports the therapeutic potential of this compound for the treatment of COPD.

Supporting Information Available: Details of syntheses and assays and characterization of all compounds. This material is available free of charge via the Internet at http://pubs.acs.org.

References

(1) Pauwels, R. A.; Rabe, K. F. Burden and clinical features of chronic obstructive pulmonary disease (COPD). *Lancet* **2004**, *364*, 613–620.

(2) Skrepnek, G. H.; Skrepnek, S. T. Epidemiology, clinical and economic burden, and natural history of chronic obstructive pulmonary disease and asthma. *Am. J. Managed Care* **2004**, *10*, S129–S138.

(3) Tashkin, D. P.; Celli, B.; Senn, S.; Burkhart, D.; Kesten, S.; Menjoge, S.; Decramer, M. A 4-tear trial of tiotropium in chronic obstructive pulmonary disease. *N. Engl. J. Med.* **2008**, *359*, 1543–1554.

(4) Belvisi, M. G.; Hele, D. J.; Birell, M. A. New anti-inflammatory therapies and targets for asthma and chronic obstructive pulmonary disease. *Expert Opin. Ther. Targets* **2004**, *8*, 265–285.

(5) Bergeron, C.; Boulet, L. Structural changes in airway diseases. characteristics, mechanisms, consequences, and pharmacologic modulation. *Chest* **2006**, *129*, 1068–1087.

(6) Lagente, V.; Manoury, B.; Nenan, S.; le Quement, C.; Martin-Chouly, C.; Boichot, E. Role of matrix metalloproteinases in the devlopment of airway inflammation and remodeling. *Braz. J. Med. Biol. Res.* **2005**, *38*, 1521–1530.

(7) Shapiro, S. D.; Kobayashi, D. K.; Ley, T. J. Cloning and characterization of a unique elastolytic metalloproteinase produced by human alveolar macrophages. *J. Biol. Chem.* **1993**, *26*, 23824–23829.

(8) Hautamaki, R. D.; Kobayashi, D. K.; Senior, R. M.; Shapiro, S. D. Requirement for macrophage elastase for cigarette smoke-induced emphysema in mice. *Science* **1997**, *277*, 2002–2004.

(9) Leclerc, O.; Lagente, V.; Panquois, J.; Berthelier, C.; Artola, M.; Eichholtz, T.; Bertrand, C. P.; Schmidlin, F. Involvement of MMP-12 and phosphodiesterase type 4 in cigarette smoke-induced inflammtion in mice. *Eur. Respir. J.* **2006**, *27*, 1102–110.

(10) Churg, A.; Wang, R. D.; Tai, H.; Wang, X.; Xie, C.; Dai, J.; Shapiro, S. D.; Wright, J. L. Macrophage metalloelastase mediates acute cigarette smoke-induced inflammation via tumor necrosis factor-a release. *Am. J. Respir. Crit. Care Med.* **2003**, *167*, 1083–1089.

(11) Wu, J.; Rush, T. S.; Hotchandani, R.; Du, X.; Geck, M.; Collins, E.; Xu, Z. B.; Skotnicki, J.; Levin, J. I.; Lovering, F. E. Identification of potent and selective MMP-13 inhibitors. *Bioorg. Med. Chem. Lett.* **2005**, *15*, 4105–4109.

(12) Markus, M. A.; Dwyer, B.; Wolfrom, S.; Li, J.; Li, W.; Malakian, K.; Wilhelm, J.; Tsao, D. H. H. Solution structure of wild-type human matrix metalloprotease 12 (MMP-12) in complex with a tight-binding inhibitor. *J. Biomol. NMR* **2008**, *41*, 55–60.

(13) Hu, Y.; Xiang, S.; DiGrandi, M. J.; Du, X.; Ipek, M.; Laakso, L. M.; Li, J.; Li, W.; Rush, T. S.; Schmid, J.; Skotnicki, J. S.; Tam, S.; Thomason, J. R.; Wang, Q.; Levin, J. I. Potent, selective and orally bioavailable matrix metalloproteinase-13 inhibitors for the treatment of osteoarthritis. *Bioorg. Med. Chem.* **2005**, *13*, 6629–6644.

(14) Li, J.; Rush, T. R.; Li, W.; DeVincentis, D.; Du, X.; Hu, Y.; Thomason, J. R.; Xiang, S.; Skotnicki, J. S.; Tam, S.; Cunningham, K. M.; Chockalingam, P. S.; Morris, E. A.; Levin, J. I. Synthesis and SAR of highly selective MMP-13 inhibitor. *Bioorg. Med. Chem. Lett.* **2005**, *15*, 4961–4966.

(15) For DBF as a scaffold for PDE4 inhibitors, see the following: Kodimuthali, A.; Jabaris, S. S. L.; Pal, M. Recent advances on phosphodiesterase 4 inhibitors for the treatment of asthma and chronic obstructive pulmonary disease. *J. Med. Chem.* **2008**, *51*, 5471–5489, and references cited therein. For MMP inhibitors, see the following: O'Brien, P. M.; Picard, J. A.; Sliskovic, D. R.; White, A. D. Method of Inhibiting Matrix Metalloproteases. U.S. Patent 6906092, 2005.

(16) Takashi Keumi, T.; Tomioka, N.; Hamanaka, K.; Kakihara, H.; Fukushima, M.; Morita, T.; Kitajima, H. Positional reactivity of dibenzofuran in electrophilic substitions. *J. Org. Chem.* **1991**, *56*, 4671–4677.

(17) Mitsumori, S.; Tsuri, T.; Honma, T.; Hiramatsu, Y.; Okada, T.; Hashizume, H.; Inagaki, M.; Arimura, A.; Yasui, K.; Asanuma, F.; Kishino, J.; Ohtani, M. Synthesis and biological activity of various derivatives of a novel class of potent, selective, and orally active prostaglandin D2 receptor antagonists. 1. Bicyclo[2.2.1]heptane derivatives. *J. Med. Chem.* **2003**, *46*, 2436–2445.

(18) Nenan, S.; Lagente, V.; Planquois, J.; Hitier, S.; Berna, P.; Bertrand, C. P.; Biochot, E. Metalloelastase (MMP-12) induced inflammatory response in mice airways: effects of dexamethasone, rolipram and marimastat. *Eur. J. Pharmacol.* **2007**, *559*, 75–81.

(19) Li, W.; Li, J.; Wu, Y.; Tam, S.; Mansour, T. S.; Sypek, J. P.; Mcfayden, I.; Hotchandani, R.; Wu, J. Preparation of Tricyclic Compounds as Matrix Metalloprotease Inhibitors. PCT Int. Appl. WO 2008057254 A2, 2008.